Spinning to a Different Beat: ^{19}F Agents for "Hot-Spot" Cellular MR Imaging

Edyta Swider and Mangala Srinivas

1 Introduction

The imaging of cellular therapeutics plays a significant and vital role in the development, optimization, and personalization of such therapy, as it can provide essential information on cell localization, number, and functionality (Fig. 1a), thus allowing dosage and delivery optimization, among others. Magnetic resonance imaging (MRI) is an anatomic and functional imaging technique which excels at soft-tissue imaging, without limitations on penetration depth. MRI is one of the commonly used imaging modalities due to its excellent safety, noninvasive nature, high resolution, lack of ionizing radiation, and intrinsic anatomic contrast. Standard (i.e. most commonly used) MRI focuses on the detection of differences in relaxation rates of the protons (^{1}H) in mobile water molecules in various tissues. However, it is normally not possible to distinguish specific therapeutic cells from their surrounding cellular milieu without the use of a specific label for the relevant cells. There have been several approaches to develop contrast agents (CAs) to improve contrast, e.g., gadolinium or superparamagnetic iron oxide (SPIO). However, metal CAs can be toxic, may not allow proper cell quantification, and often require "before" and "after" images to detect changes in contrast. Only SPIO-based agents have been used in the clinic for cell tracking [1] and these agents are no longer commercially available.

E. Swider • M. Srinivas (✉)
Department of Tumor Immunology, Radboud Institute for Molecular Life Sciences, Radboud University Medical Center, Nijmegen, The Netherlands
e-mail: mangala.srinivas@radboudumc.nl

J.W.M. Bulte, M.M.J. Modo (eds.), *Design and Applications of Nanoparticles in Biomedical Imaging*, DOI 10.1007/978-3-319-42169-8_7

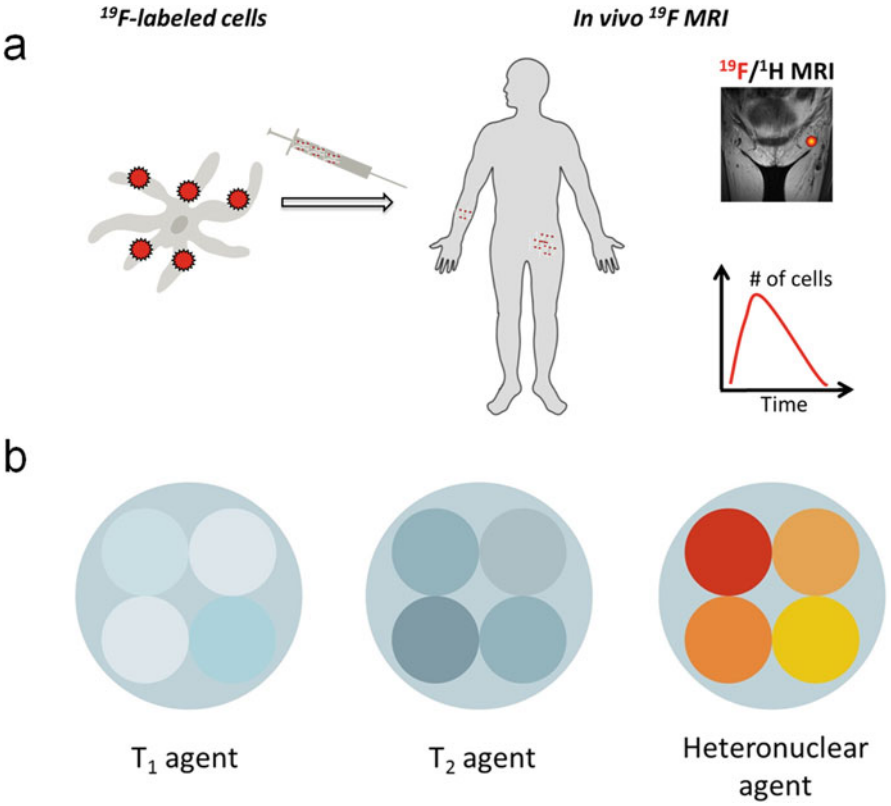

Fig. 1 General ^{19}F MRI cell labeling. (**a**) A general protocol for ^{19}F MRI of labeled cells involves ex vivo labeling of the cells, transfer to the subject, and then imaging. A smaller number of studies use direct in vivo labeling, typically macrophages. (**b**) "Hot-spot" imaging. The figure demonstrates the images typically obtained with T_1, T_2 contrast agents, and a ^{19}F label. The contrast agents change the contrast in the anatomic (^{1}H) scan, while the ^{19}F image must be acquired separately, rendered in false color, and is then typically superimposed over the standard anatomic scan (in *gray* scale). Thus, the detection of ^{19}F signal is less ambiguous, and, more importantly, the signal intensity directly relates to agent concentration, given sufficient signal to noise. In practice, this means that the cell numbers can be estimated directly from image data, one of the main advantages of the technique

In the last decade, "hot-spot" imaging has gained a lot of attention. Hot-spot imaging is hetero-nuclear MRI using ^{13}C, ^{23}Na, ^{31}P, or ^{19}F in addition to ^{1}H, which enables direct detection rather than indirect, as is the case for CAs (Fig. 1b). Out of these four elements, ^{19}F has been the main focus as it is essentially absent in biological tissues; thus there is no endogenous background signal, which makes it more attractive for hot-spot imaging [2]. One clear example of the advantage of the lack of background signal is a recent paper using ^{19}F MRI to track inflammatory macrophages and monocytes in a murine model of multiple sclerosis [3]. Here the inflammatory cells were found not only in the diseased

spinal cord, as expected, but also in neighboring bone marrow tissue. This ability to locate ^{19}F signal even in unexpected locations without comparison to a "before" image, given a sufficient signal-to-noise ratio, is one of the key advantages of the technique.

^{19}F MRI has been applied as a powerful imaging tool for diverse applications, such as cell tracking [4], drug metabolism, plaque detection, and monitoring inflammation. Cell tracking using ^{19}F MRI has been applied to various cell types, such as dendritic cells (DCs), T cells, stem cells, and macrophages [5]. In order to distinguish relevant cells from the background, they need to be labeled with fluorinated labels, described in the following section.

2 Fluorocarbons

2.1 General Properties of Fluorine

Using fluorine in MRI has several advantages as ^{19}F is a spin ½ nucleus, which means that it has an odd number of protons and neutrons and spherical charge distribution, and a gyromagnetic ratio close to the proton. Thus, for a given magnetic field value, the spin processes at almost the same frequency, permitting the use of a conventional proton spectrometer to detect fluorine [6]. Fluorine has 100 % natural abundance and an extremely broad chemical shift and is not naturally present in biological tissues and therefore has no biological background signal; the traces of fluorine in bone and teeth exhibit a very short spin-spin relaxation time (T_2) and are not visible to conventional MRI methods [2]. In all, fluorine MRI gives a very high contrast-to-noise ratio and specificity, in a situation where a fluorinated element is introduced as a contrast agent. Such agent requires a very high density of ^{19}F nuclei on the molecule in addition to a high tissue concentration in order to produce an image quality such as the one of ^{1}H MRI. However, it is important to realize that the administered levels of ^{19}F will still be many orders of magnitude lower than the amount of ^{1}H present in biological tissues, and thus, despite all its advantages in terms of imaging properties, the low concentrations of ^{19}F frequently result in images that hover at the detection limit with low signal-to-noise ratios (SNRs). Finally, some fluorocarbons show a T_1 sensitivity to oxygen tension, which may allow its use as an in vivo sensor [2]; alternatively, this T_1 variability can be a nuisance, hindering accurate quantification.

2.2 Fluorinated Compounds/Molecules

An example of fluorinated compounds includes fluorinated peptides, polymers, and also fluorinated small molecules, such as sugars; however these result in much lower cell loading and, as a result, a lower detection sensitivity. Small fluorinated

molecules have lower ^{19}F content than larger fluorocarbons, such as perfluorocarbons (PFCs); however their advantage is that they can be used to study cell functionality [5]. Despite this benefit, the insufficient sensitivity of the small molecules makes them less attractive for in vivo use. Recent developments in small fluorinated molecules include fluorinated albumin [7] and self-assembling nanoparticles sensitive to their environment [8], although neither of these have been applied to cell tracking. Some examples are listed in Table 1.

There have been limited studies using fluorinated drugs (see Table 1). The limit here is the high reactivity and electronegativity of fluorine, which when incorporated into a drug can significantly alter drug chemistry and subsequent metabolism. Chemical shift artifacts can also be an issue. For all these reasons, such small molecules are seldom used for cell tracking.

2.3 Perfluorocarbons

Perfluorocarbons (PFCs) are synthetic molecules mainly composed of carbon and fluorine atoms (see Table 2 for a summary of their physical properties). Depending on their chemical structure and molecular weight, PFCs exist in a gaseous, liquid, or even solid form. The compounds are extremely stable, generally have low vapor pressures, and are inert. PFCs do not react with living tissues due to their carbon-fluorine bonds, which cannot be metabolized in vivo, and they have low intermolecular forces, and hence, the surface tension of the liquid form of PFCs is extremely low. Most PFCs have a surface tension of 14–18 dyne/cm [9]. As gases, PFCs show some toxicity, while in a liquid form they are relatively safe [10]. Clearance of PFC agents from the body generally occurs via the mononuclear phagocyte system (MPS) uptake (phagocytic cells primarily in lymph nodes, spleen, and liver) and finally lung exhalation. Some PFCs can also bind and dissolve oxygen. This led to their early use as blood substitutes, although the idea has been commercially abandoned. PFCs are still used clinically, for example for partial liquid ventilation [LiquiVent, Alliance Pharmaceutical Corporation], eye surgery [Perfluoron™, Alcon® Inc., USA], and as ultrasound contrast agents as gas bubbles [Sonovue®, Bracco International B.V.] (Fig. 2a).

PFCs have now found their use as imaging labels for ultrasonography, computed tomography, and ^{19}F MRI. Their use in the latter imaging method is especially beneficial, as PFCs have a high payload of fluorine atoms, which makes ^{19}F MRI a promising modality for in vivo quantitative imaging, including in vivo cell tracking. Here, liquid PFCs are more suitable, as they result in the most favorable imaging characteristics.

For imaging purposes, PFCs offer a high ^{19}F density per molecule, and thus high sensitivity, provided that multiple fluorine resonances do not occur. To avoid such chemical shift artifacts, PFCs such as ring ethers or longer linear ether chains are frequently used [5, 11]. The most frequently used ^{19}F MRI labels consist of perfluorooctyl

Table 1 Overview of different ^{19}F labels, cell types, and cell loading

Major ^{19}F component	Additives	Hydrodynamic diameter (nm)	Cell type	Average cell loading ($\times 10^{12}$ ^{19}F atoms/cell)	No. of (dominant) resonances	Ref.
Various PFCs	Atto 647	200–300	Primary human DCs	30	1	[22]
PFCE PFOB		233 224	Primary human stem/ progenitor cells	20 0.5	1 Multiple	[33]
PFCE	Dye		Rodent glioma	0.2	1	[34]
PFOB	Drug	225	Primary human umbilical cord smooth muscle cells		Multiple	[35]
Various PFCs	Fluorinated quantum dots	200	Murine macrophage Human carcinoma		Multiple	[36]
PFCE	Targeting peptide	170	Human umbilical cord vein Endothelial cells		1	[37]
PFOB	Targeting antibody Transfection agent		Human cancer cell lines		Multiple	[38, 39]
PFCE	Dye	145	Macrophages		1	[40]
Hyperbranched fluorinated polymer	Drug	20–30	Human glioblastoma cell line	0.0005	1	[41]
PERFECTA	n/a	140–220	Dendritic cells	19.2	1	[14]
Fluorinated colchicine derivatives	n/a	n/a	Human leukemia cell line		Multiple	[42]
Fluorinated reporter molecules	n/a	n/a	Various, including bacteria and human cancer cell lines			[43–45]
Fluorinated prodrug			Human cancer cell lines			[46]

Reproduced with permission from Ref. [5]

Table 2 General physical properties of various PFCs used in cell tracking

Perfluorocarbon	Formula	Molecular weight	Density (g/mL)	Boiling point (°C)
Perfluoropentane	C_5F_{12}	288	1.62	26–36
Perfluorohexane	C_6F_{14}	338	1.76	58–60
Perfluorooctyl bromide	$C_8F_{17}Br$	499	1.93	140.5
Perfluorononane	C_9F_{20}	488	1.80	126
Perfluorodecalin	$C_{10}F_{18}$	462	1.99	144
Perfluoro-15-crown-5-ether	$C_{10}F_{20}O_5$	580	1.78	145
PERFECTA	$C_{21}H_8F_{36}O_4$	1008	2.09	ND

bromide (PFOB), perfluoro-15-crown-5-ether (PFCE), and a linear PFPE polymer mixture, which is commercialized as Cell Sense (Celsense Inc., Pittsburgh PA, USA). Characteristics of examples of these PFCs are shown in Table 1, while Fig. 2b shows the structure of PFCE, PFOB, and PFPE.

PFCs have a unique and sometimes undesirable characteristic, in that they are fluorophilic, i.e., simultaneously lipophobic and hydrophobic (Fig. 2b). Consequently, PFCs separate when placed in an aqueous environment and are immiscible in cell membranes. Because of this, they require emulsification, to form nanoemulsions, or entrapment into particles to achieve stability in biological environments. In such forms, PFCs can also be used to label cells for in vivo cell tracking.

3 ^{19}F MRI Labels

The ideal ^{19}F label needs to have certain characteristics, described in more detail elsewhere [2]. Briefly, such an agent has to be biologically inert and chemically stable. Fluorinated compounds should be nontoxic for the host and have minimal impact on labeled cell function. The label needs to be suitable for cell uptake, with smaller droplets or particles for intracellular labeling and potentially larger ones for blood pool imaging. What is more, cells need to take up sufficient amounts of the label in order to be detected (ranging from 0.5 to 30×10^{12} ^{19}F atoms/cell) [5]. The "sufficient amount" is based on the number of cells per voxel and T_1 and T_2 characteristics of the compound. Last, but not least, the ^{19}F compounds must have beneficial relaxation parameters, with a short T_1 and a long T_2 [2]. Typical labels are composed of a fluorinated molecule and a coating or surfactant which stabilizes the fluorocarbon to make it more suitable for cell labeling and cell uptake (Fig. 3).

In general, high signal density per molecule is necessary. Therefore, most labels consist of fluorocarbon or even liquid PFCs such as perfluoropolyethers (PFPE), typically administered as nanoemulsions with droplet sizes around 100–300 nm. Due to their poor miscibility, PFCs need to be "packaged" to stabilize them in aqueous biological environments. These packaging techniques are discussed in the following section.

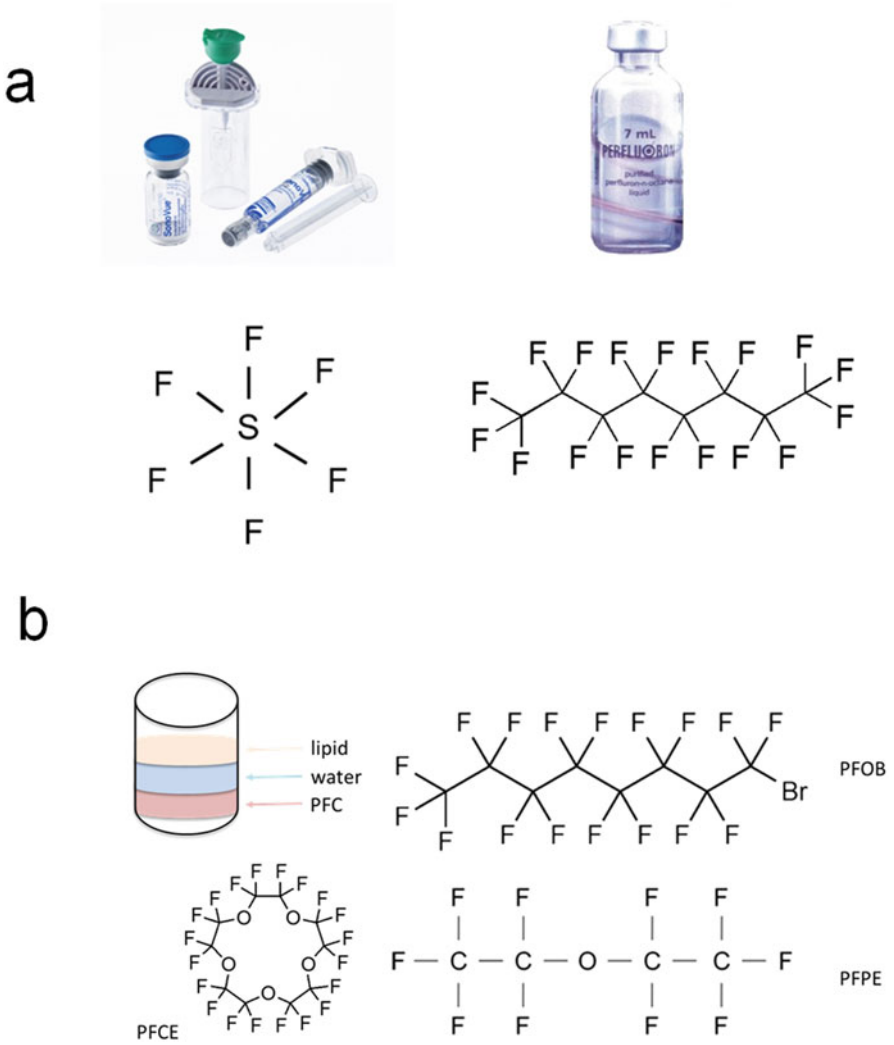

Fig. 2 Perfluorocarbons. (**a**) PFCs are currently in clinical use, as both gases and liquids. Shown is an ultrasound microbubble contrast agent containing sulfur hexafluoride gas (Sonovue®) and a perfluorooctane liquid used in eye surgery (Perfluoron™). (**b**) Most cell labels are perfluorocarbons (PFCs), polymers of carbon and fluorine. These compounds have unique properties; in particular they mix with neither aqueous nor organic solvents. Some of the more commonly used PFCs for cell tracking are PFOB, PFCE, and PFPE, shown here

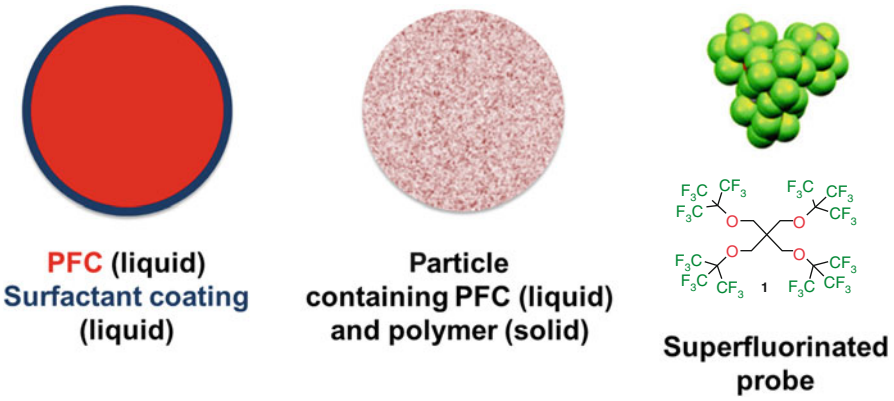

Fig. 3 PFCs stabilized for cell labeling. PFCs, being simultaneously hydrophobic and lipophobic, must be stabilized for use in aqueous environments. Most often, this is done using emulsion droplets, where a liquid PFC is coated with a liquid surfactant. Some groups work with particles, containing a liquid PFC in a solid polymer. The final option is a large fluorinated molecule. Reproduced with permission from Ref. [14]

3.1 Label Formulation: "PFC Packaging"

Cell tracking applications require PFCs to be formulated into a biocompatible label. There are several methods to formulate fluorinated labels. The route of synthesis depends on the type of label, its size, properties, and addition of extra molecules, e.g., fluorescent dyes. Emulsions are prepared via emulsification processes using, e.g., sonication or microfluidization. Emulsions should have a small, uniform droplet size, ideally smaller than 200 nm, as larger droplets may affect cell activation phenotype post-labeling [11]. However, the poor affinity between the PFC, surfactant, and aqueous continuous phase can limit emulsion stability. Furthermore, it can be difficult to add additional agents such as fluorescent dyes, drugs, or antibodies without changing the emulsion properties. Furthermore, the addition of extra moieties to an emulsion can result in separation of those moieties from PFC in the cell or in vivo, with no assurance of their localization. Recently, nanoparticles have received a lot of interest [5, 12], due to their enhanced stability. A key advantage of using particles is that the components of the particles can be modified without altering the formulation protocol.

3.2 Emulsions

Emulsions are the simple product of vigorously mixing oil and water. More specifically, an emulsion is a suspension of two immiscible liquids. In the literature, emulsion droplets are frequently referred to as "particles" but to avoid confusion,

here particles are defined as solids which can be isolated from and added back to the continuous phase (water or buffer) without undergoing changes other than hydration, with the particles being able to be stored as powder. Emulsion droplets cannot be isolated in such fashion without losing stability.

Emulsions are the most commonly used cell labels due to their high content of PFCs per droplet and simplicity of production. Emulsions consist of an immiscible compound that is surrounded by a surfactant. The role of the surfactant is to stabilize the formed droplets in the continuous phase (water) and delay the PFC from settling out and coalescing to form a separate layer. PFC emulsions for MRI generally exhibit poor stability due to the fact that the surfactant used cannot be miscible with both the PFC and water, unless it is a fluorinated surfactant. Fluorinated surfactants are avoided, due to the potential for toxicity and the chemical shift artifacts that can result from the added fluorine. PFC emulsions are described in more detail elsewhere [13].

Recently a new compound called PERFECTA has been developed as a ^{19}F MRI tracer. PERFECTA is a superfluorinated molecular probe suitable for in vivo cell tracking. It has high detection sensitivity, a single, sharp resonance peak, and attractive T_1 and T_2 values [14]. PERFECTA is not fully fluorinated, but has a hydrocarbon polar core and four ether bonds, which might undergo enzymatic degradation in vivo. Most other recent studies have focused on conventional, existing PFCs [12, 15–17]. Figure 3 shows a representation of an emulsion droplet, a nanoparticle, and a large fluorinated molecule.

3.3 Micelles

Micelles are lipid-based compounds composed of amphiphilic molecules that undergo spontaneous self-assembly in an aqueous solution. This spontaneous self-assembly is due to the amphipathic nature of the molecule. To form a micelle, the amphiphilic molecules arrange in a way where the hydrophobic groups create a core, while the hydrophilic groups are on the outside and have contact with water [18]. The size of micelles ranges from 2 to 20 nm, and it depends on their composition, modifications, and concentration. There have been several studies incorporating a hydrophilic Gd(III) chelate into micelles for in vivo imaging [19–21] to enhance the T_1 MRI contrast. Micelles can be further modified with groups that bind to specific targets.

3.4 Dendrimers

Dendrimers are nanoscale macromolecules that have well-defined polymeric chains which branch off from a central core. They can be functionalized with polyfluorinated groups and targeting moieties. Dendrimers modified with Gd(III) chelate

show increase in rotational correlation times which leads to strong enhancement in T_1 relaxation rates when compared to lower molecular weight chelates [18]. Dendrimers typically present prolonged retention times within the vascular system in comparison to lower molecular weight chelates, which usually undergo a fast renal clearance.

Dendrimers are very appealing in ^{19}F MRI label design due to large number of surface functional groups which can be reacted with polyfluorinated precursors, leading to materials with potentially high concentrations of fluorine nuclei [18]. However, it is possible that dendrimers may be metabolized in vivo leading to potentially toxic compounds. In general, less is known about these extremely large molecules and their in vivo behavior.

3.5 PFC Nanoparticles

Particles are an attractive alternative for ^{19}F MRI compared to conventional liquid emulsion droplets, as they are more stable and can be frozen as a dry powder for easy storage and transport [5]. PFC nanoparticles typically consist of a PFC entrapped in a solid polymer. We previously reported on stable encapsulation of PFC in poly(D,L-lactide-*co*-glycolide acid) (PLGA) particles [22]. The PFC-PLGA particles were prepared using single-emulsion solvent-evaporation method. In this method, the polymer is dissolved in an organic solvent, and the PFCE is added. Next, this organic phase is added to an aqueous solution containing surfactant under sonication. The role of surfactant is to stabilize the cells and prevent Ostwald ripening (which is very common in emulsions, including PFC emulsions) [23]. Sonication is then followed by solvent evaporation, and washing and freeze-drying of particles. After the last step, particles can be stored in a powder form for extended periods of time. PLGA-PFC particles can be easily modified with targeting ligands, and fluorescent dyes, and they can also be used to encapsulate drugs.

There are several methods to characterize PFC nanoparticles, for example dynamic light scattering, electron microscopy, and nuclear magnetic resonance (NMR). The first two methods are used to study diameter, while ^{19}F NMR is used to measure fluorine content. PFC particles prepared with solvent evaporation method typically have a diameter of 200 nm, comparable to many PFC emulsion droplets.

4 Cell Labeling

Most of the studies performed thus far in this field have used naturally phagocytic cells, such as macrophages or DCs. These types of cells readily phagocytose label droplets or particles, generally resulting in labeling in the order of 10^{10}–10^{13} fluorine atoms per cell (see Table 1).

A general cell labeling protocol is shown in Fig. 4. Key labeling steps include the length of time the cells are incubated with the label, the concentration of the label, and removal of excess label. Label uptake can be encouraged when necessary through the use of positive changes on the labels, such as through transfection agents [24]. It is important to show that the label is incorporated in a stable manner within the cell, and will remain within the relevant cell in vivo. In addition, it needs to be ensured that any excess label is removed through careful washing steps before transfer to the subject.

It is also necessary to balance the uptake of label with any effects on cell functionality and cytotoxicity. In particular, it is vital to assess any effect of the label on cell migration and other functions that are necessary in vivo. It has been shown that iron oxide labeling can alter cell migration in neural stem cells [25], although another study that exhaustively compared various labels including iron oxide and ^{19}F did not find any effect in mesenchymal stem cells [26]. Thus, the effect of labeling appears to be cell dependent and label dependent at the very least. Furthermore, with some fluorine labels, cell migration is known to be unaffected, and ^{19}F MRI has in fact been suggested as a cell migration assay for larger cell numbers [27]. However, one cannot assume that any particular label will not affect migration, or any particular function, in a different cell type, i.e., each cell type-label pair needs to be individually optimized and thoroughly characterized.

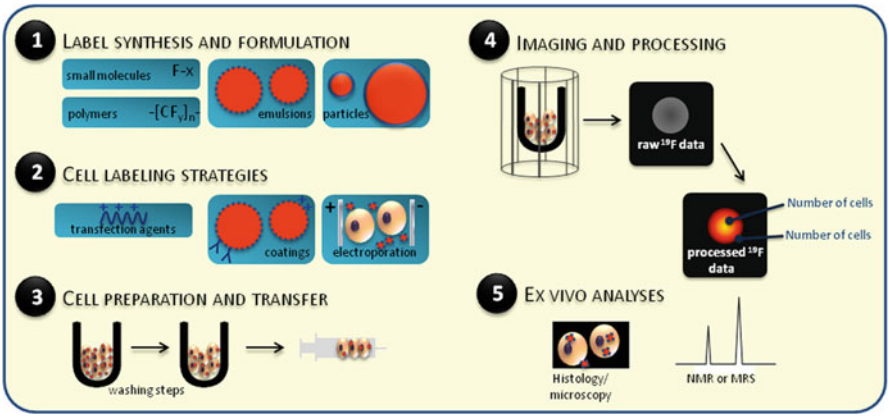

Fig. 4 Typical ex vivo cell labeling protocol. Key steps in cell labeling for ^{19}F MRI. The figure shows the most commonly used protocols for each step; variations proposed in the literature are discussed in the text. Appropriate selection of label and labeling protocol is crucial for success of the experiment (Step 1). Cell labeling (Step 2) may require enhancement through the use of coatings or transfection agents. After suitable preparation (Step 3) the cells can be imaged. Post-processing leads to quantification (Step 4). Finally, image post-processing can be carried out (Step 5) to corroborate the in vivo data. Reproduced with permission from Ref. [5]

In all cases, quantification of cell numbers is much more accurate when cells are labeled ex vivo, as the average ^{19}F content per cell can be readily determined. When the label is injected systemically [28] in vivo, and subsequently taken up by target cells (typically macrophages), quantification becomes more complex, as the label uptake per cell cannot be determined. Even with ex vivo-labeled cells, the label can be lost or transferred to other cell types, particularly macrophages present within the surrounding host tissue. For example, labeled mesenchymal stem cells lost their ^{19}F agent to bystander macrophages by 17 days after transfer [29]. Thus, the signal detected could be falsely interpreted at later time points. Such label transfer may vary depending on cell type, label type, transfer site, division status of the cells, and various other factors. Similar results were also obtained in another study [30], where transgenic neural stem cells expressing a bioluminescence marker were also labeled with a fluorinated agent. Here, the ^{19}F signal was retained for at least several days after the bioluminescence signal was lost, and indicator of cell death (Fig. 5). This slow loss of ^{19}F signal even after cell death could be a result of various factors including the particular properties of the label or cell, or simply slow clearance from the brain. Regardless, these studies highlight that the interpretation of cell tracking can become more complex after its initial stages.

The fate of the agent, both in cells and in vivo, is an important consideration, particularly in terms of any toxicity and the clearance rate and route. This may be less of an issue if cells are prelabeled ex vivo before injection to the subject, as then only very small amounts of PFCs are administered. However, in cases where cells are labeled in vivo, after systemic injection of the agent, retention and clearance are important considerations [31] (Fig. 6). In one study, it was found that the biological half-life of different PFCs administered as emulsions varied from 9 days to over 250 days. However, the influence of the type of label, surfactant used, site of injection, and other factors is not clear.

5 Recent Developments

5.1 Multicolor ^{19}F MRI

The broad chemical shift of ^{19}F allows the possibility of imaging well-separated resonances. Multiple resonances are most often a drawback, as they represent "lost" ^{19}Fs that do not contribute to the signal, or that create artifacts making the image "fuzzy" (Fig. 7). However, in some cases this drawback can be harnessed to image multiple cell lines at different resonance frequencies. Recently, this has been applied to different therapeutic cell subsets, which were labeled with different PFCs (PFO and PFCE, respectively) [12] (Fig. 8). A standard gradient-echo sequence was used for imaging, where the excitation peak was sufficiently broad so as to excite both the main

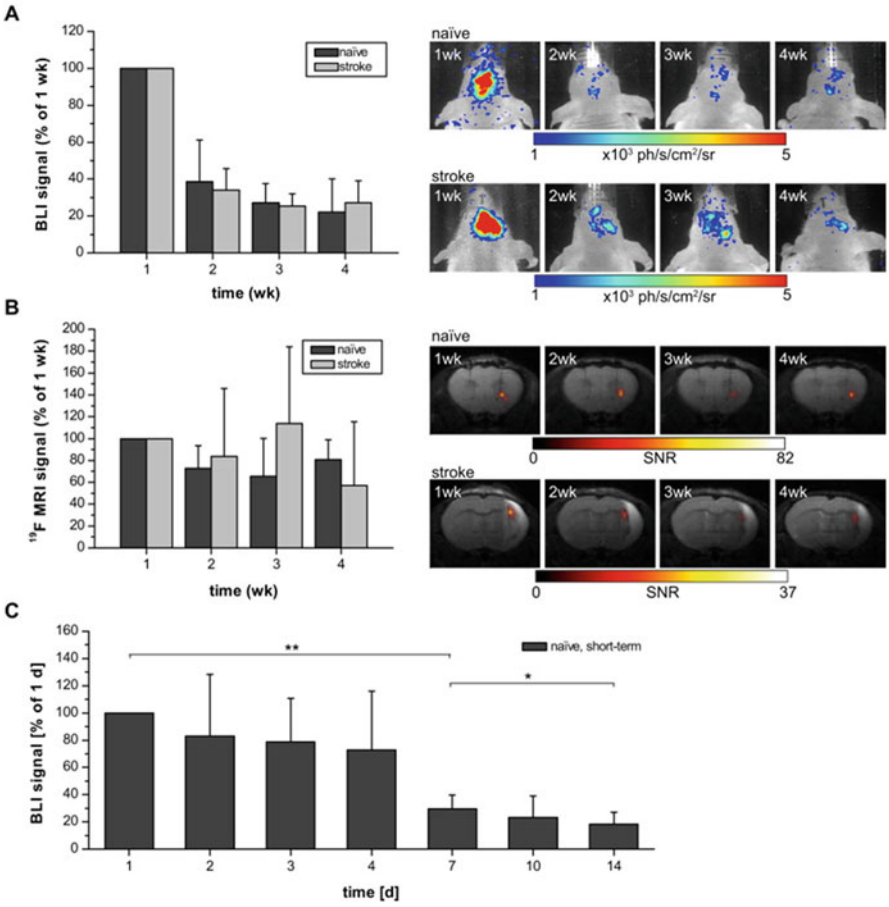

Fig. 5 ^{19}F MRI signal can persist even after cell death in some cases. BLI and ^{19}F MRI signal after implantation of neural stem cells into naïve mice and stroked animals that underwent middle cerebral artery occlusion (MCAO) 48 h earlier. (**a**) BLI signal in naïve ($n=5$) or stroked ($n=4$) animals decreased rapidly over 4 weeks indicating impaired graft survival. (**b**) ^{19}F SNR in naïve and stroked animals persisted, with more scatter in the stroke group. (**c**) To better resolve the decrease in BLI signal, a separate group of naïve animals ($n=6$) underwent BLI one day after implantation and up to 2 weeks after. The onset of decreased graft survival was found at 7 days. */**: Significance level $p \leq 0.05/0.01$, all values presented as mean ± standard deviation. Reproduced with permission from Ref. [30]

resonance of the PFO and the single resonance of the PFCE. Both were detected simultaneously, but due to the known bandwidth per voxel, the signals could be separated. The technique clearly has limitations, for example, in applications where the cell distribution is very complex. Still, it allows imaging of two cell populations simultaneously. Such work has also been carried out with stem cells, using spectroscopic imaging [32].

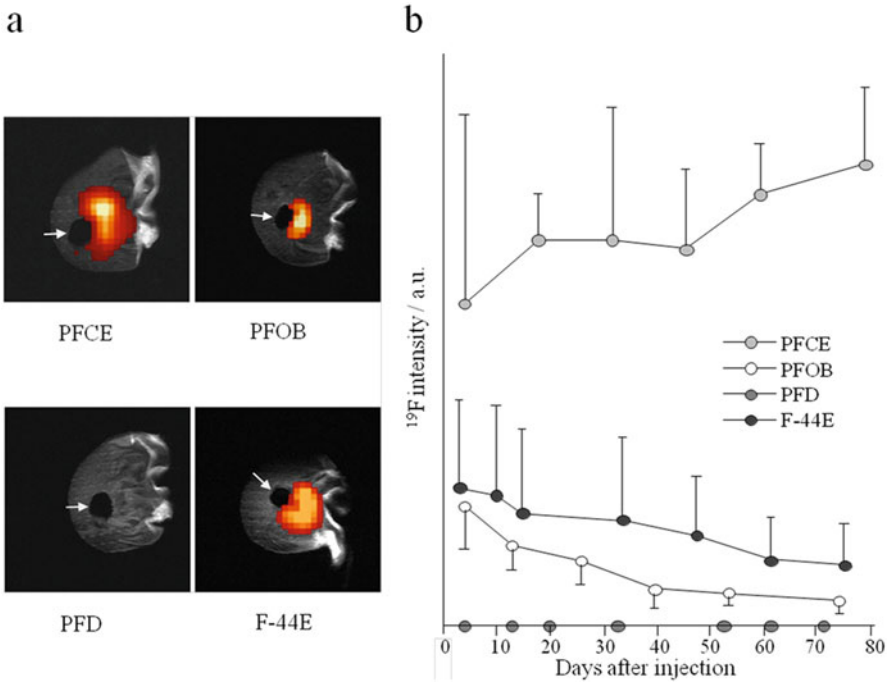

Fig. 6 Retention and sensitivity of different PFCs. In vivo ^{19}F chemical shift imaging signal in the ear after induction of inflammation by ear clipping (holes marked by *arrows*) and subsequent injection of 500 μL perfluorocarbon (PFC) emulsion ($n=4$ animals for each PFC). (**a**) Overlay of ^{19}F signal and anatomical scan for the initial MR measurement 3–4 days after PFC injection. (**b**) Time course of the fluorine signals for the different PFCs. F-44E, trans-bis-perfluorobutyl ethylene; PFCE, perfluoro-15-crown-5 ether; PFD, perfluorodecalin; PFOB, perfluorooctyl bromide. Reproduced with permission from Ref. [31]

5.2 Multimodal Imaging

No single imaging modality is perfect and able to provide all the necessary answers with certainty. In fact, nowadays the majority of ^{19}F cell tracking imaging studies use multimodal imaging, most often combining MRI with fluorescence, either in vivo or ex vivo using histopathology. The advantages of multimodal cell tracking include verification of data obtained using a new imaging agent or technique with an established one, and the ability to gather complementary information from a single experiment.

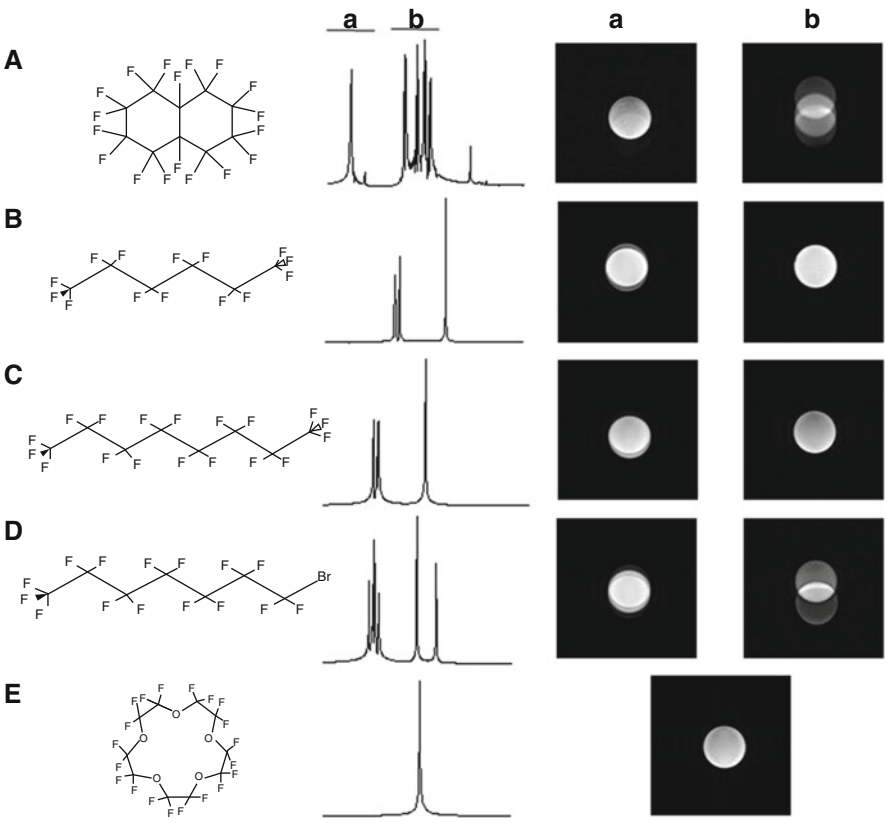

Fig. 7 Chemical shift artifact. The ^{19}F NMR spectrum, chemical structure, and the ^{19}F MR images are shown. The acquisition frequency of the MR images was centered on each peak or group of peaks, and the corresponding image is shown (indicated by **a** and **b**). (**a**) Perfluorodecalin ($C_{10}F_{18}$) has several peaks in the ^{19}F spectrum. It is used in commercial oxygen carriers and blood pool agents. (**b**) Perfluorohexane (C_6F_{14}) is also used as a contrast agent for ultrasound imaging. (**c**) Perfluorooctane (C_8F_{18}) is also used as an oxygen carrier. (**d**) Perfluorooctylbromide (C_8BrF_{17}), or PFOB, is a blood substitute that has also been used for ^{19}F MRI. However, the presence of multiple ^{19}F resonances complicates the imaging process. (**e**) Perfluoro-15-crown ether ($C_{10}F_{20}O_5$) has 20 equivalent ^{19}F atoms, resulting in a single resonance peak. The compound has been used for ^{19}F MRI for cell tracking and as an oxygen sensor. Reproduced with permission from Ref. [22]

6 Conclusions and Future Outlook

^{19}F MRI for cell tracking has recently been demonstrated in the clinic [15]; thus its clinical applicability is no longer in dispute. There is still no consensus on which PFC, if any, is the best for in vivo application, particularly in terms of balancing imaging favorability with retention times, and new and more "ideal" compounds are continually being generated. Furthermore, the relatively long imaging times necessary and limited availability of suitable hardware to do ^{19}F MRI are still a

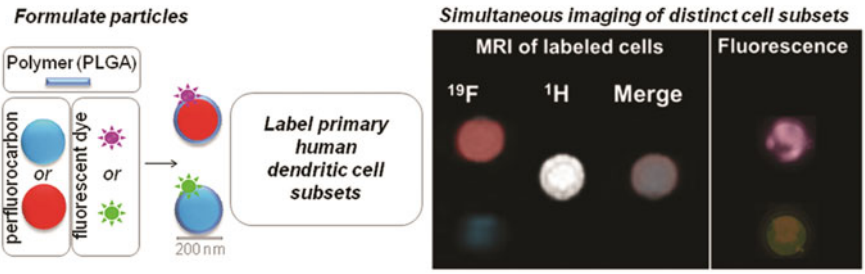

Fig. 8 Imaging multiple resonance frequencies. In some cases, the chemical shift can be used to image distinct fluorinated compounds separately. In this example, PLGA nanoparticles were formulated with different PFCs (here shown in *blue* or *red*), and different fluorescent dyes (*purple* or *green*). The resultant particles were used to label primary human therapeutic cells, which were then imaged. The ^{19}F image shows two signals, due to the two resonance frequencies, which can then be resolved in line with the ^{1}H image. Fluorescence images are also shown. Reproduced with permission from Ref. [12]

hindrance for the broad application of ^{19}F MRI. Regardless, given all the advantages and unique possibilities outlined briefly in this chapter, the future of "hot-spot" imaging, particularly for cell tracking, is getting hotter.

Acknowledgment This work was supported by the European Research Council (ERC) Starting Grant (CoNQUeST Grant no. 336454) to MS.

References

1. de Vries IJ et al. Magnetic resonance tracking of dendritic cells in melanoma patients for monitoring of cellular therapy. Nat Biotechnol. 2005;23(11):1407–13.
2. Srinivas M, Heerschap A, Ahrens ET, Figdor CG, de Vries IJ. 19F MRI for quantitative in vivo cell tracking. Trends Biotechnol. 2010;28.
3. Zhong J, Narsinh K, Morel PA, Xu H, Ahrens ET. In vivo quantification of inflammation in experimental autoimmune encephalomyelitis rats using fluorine-19 magnetic resonance imaging reveals immune cell recruitment outside the nervous system. PLoS One. 2015;10(10).
4. Ahrens ET, Flores R, Xu H, Morel PA. In vivo imaging platform for tracking immunotherapeutic cells. Nat Biotechnol. 2005;23.
5. Srinivas M, Boehm-Sturm P, Figdor CG, de Vries IJ, Hoehn M. Labelling cells for in vivo cell tracking using 19F MRI. Biomaterials. 2012;33.
6. Diou O, Tsapis N, Giraudeau C, Valette J, Gueutin C, Bourasset F, et al. Long-circulating perfluorooctyl bromide nanocapsules for tumor imaging by 19FMRI. Biomaterials. 2012;33.
7. Chubarov AS, Zakharova OD, Koval OA, Romaschenko AV, Akulov AE, Zavjalov EL, et al. Design of protein homocystamides with enhanced tumor uptake properties for 19F magnetic resonance imaging. Bioorg Med Chem. 2015;23(21).
8. Yuan Y, Ge S, Sun H, Dong X, Zhao H, An L, et al. Intracellular self-assembly and disassembly of 19F nanoparticles confer respective "Off" and "On" 19F NMR/MRI signals for Legumain activity detection in zebrafish. ACS Nano. 2015;9(5).

9. Sarkar S, Paswan A, Prakas S. Liquid ventilation. Anesth Essays Res. 2014;8(3).
10. Cosco D, Fattal E, Fresta M, Tsapis N. Perfluorocarbon-loaded micro and nanosystems for medical imaging: A state of the art. J Fluorine Chem. 2015;171.
11. Ahrens ET, Zhong J. In vivo MRI cell tracking using perfluorocarbon probes and fluorine-19 detection. NMR Biomed. 2013;26(7).
12. Srinivas M, Tel J, Schreibelt G, Bonetto F, Cruz LJ, Amiri H, et al. PLGA-encapsulated perfluorocarbon nanoparticles for simultaneous visualization of distinct cell populations by 19F MRI. Nanomedicine. 2015;10(15).
13. Janjic JM, Ahrens ET. Fluorine-containing nanoemulsions for MRI cell tracking. Adv Rev. 2009;1(5).
14. Ilaria Tirotta, et al. A superfluorinated molecular probe for highly sensitive in vivo19F-MRI. J Am Chem Soc. 2014;136.
15. Ahrens ET, Helfer BM, O'Hanlon CF, Schirda C. Clinical cell therapy imaging using a perfluorocarbon tracer and fluorine-19 MRI. Magn Reson Med. 2014;72(6).
16. Kadayakkara DK, Damodaran K, Hitchens TK, Bulte JW, Ahrens ET. (19)F spin-lattice relaxation of perfluoropolyethers: Dependence on temperature and magnetic field strength (7.0-14.1T). J Magn Reson. 2014;242.
17. de Vries A, Moonen R, Yildirim M, Langereis S, Lamerichs R, Pikkemaat JA, et al. Relaxometric studies of gadolinium-functionalized perfluorocarbon nanoparticles for MR imaging. Contrast Media Mol Imaging. 2014;9(1).
18. Knight JC, Edwards PG, Paisey SJ. Fluorinated contrast agents for magnetic resonance imaging; a review of recent developments. RSC Adv. 2011;1.
19. Zhang G, Zhang R, Wen X, Li L, Li C. Micelles based on biodegradable poly(L-glutamic acid)-b-polylactide with paramagnetic Gd ions chelated to the shell layer as a potential nanoscale MRI-visible delivery system. Biomacromolecules. 2008;9(1).
20. Grogna M, Cloots R, Luxen A, Jérôme C, Passirani C, Lautram N, et al. Polymer micelles decorated by gadolinium complexes as MRI blood contrast agents: design, synthesis and properties. Polymer Chem. 2010;1.
21. Mouffouk F, Simão T, Dornelles DF, Lopes AD, Sau P, Martins J, et al. Self-assembled polymeric nanoparticles as new, smart contrast agents for cancer early detection using magnetic resonance imaging. Int J Nanomed. 2015;10.
22. Srinivas M, Cruz LJ, Bonetto F, Heerschap A, Figdor CG, de Vries IJ. Customizable, multifunctional fluorocarbon nanoparticles for quantitative in vivo imaging using 19F MRI and optical imaging. Biomaterials. 2010;31(27).
23. Patel SK, Williams J, Janjic JM. Cell Labeling for 19F MRI: new and improved approach to perfluorocarbon nanoemulsion design. Biosensors. 2013;3(3).
24. Srinivas M, Turner MS, Janjic JM, Morel PA, Laidlaw DH, Ahrens ET. In vivo cytometry of antigen-specific t cells using 19F MRI. Magn Reson Med. 2009;62(3).
25. Cromer Berman SM, Kshitiz, Wang CJ, Orukari I, Levchenko A, Bulte JW, Walczak P. Cell motility of neural stem cells is reduced after SPIO-labeling, which is mitigated after exocytosis. Magn Reson Med. 2013;69(1).
26. Muhammad G, Jablonska A, Rose L, Walczak P, Janowski M. Effect of MRI tags: SPIO nanoparticles and 19F nanoemulsion on various populations of mouse mesenchymal stem cells. Acta Neurobiol Exp. 2015;75(2).
27. Bonetto F, Srinivas M, Weigelin B, Cruz LJ, Heerschap A, Friedl P, et al. A large-scale (19)F MRI-based cell migration assay to optimize cell therapy. NMR Biomed. 2012;25(9).
28. Bönner F, Merx MW, Klingel K, Begovatz P, Flögel U, Sager M, et al. Monocyte imaging after myocardial infarction with 19F MRI at 3 T: a pilot study in explanted porcine hearts. Eur Heart J Cardiovasc Imaging. 2015;16(6).
29. Gaudet JM, Ribot EJ, Chen Y, Gilbert KM, Foster PJ. Tracking the fate of stem cell implants with fluorine-19 MRI. PLoS One. 2015;10(3).
30. Boehm-Sturm P, Aswendt M, Minassian A, Michalk S, Mengler L, Adamczak J, et al. A multimodality platform to image stem cell graft survival in the naïve and stroke-damaged mouse brain. Biomaterials. 2014;35(7).

31. Jacoby C, Temme S, Mayenfels F, Benoit N, Krafft MP, Schubert R, et al. Probing different perfluorocarbons for in vivo inflammation imaging by 19F MRI: image reconstruction, biological half-lives and sensitivity. NMR Biomed. 2013;27(3).
32. Partlow KC, Chen J, Brant JA, Neubauer AM, Meyerrose TE, Creer MH, et al. 19F magnetic resonance imaging for stem/progenitor cell tracking with multiple unique perfluorocarbon nanobeacons. FASEB J. 2007;21(8).
33. Mizukami S, Takikawa R, Sugihara F, Hori Y, Tochio H, Wälchli M, et al. Paramagnetic relaxation-based 19f MRI probe to detect protease activity. J Am Chem Soc. 2008;130(3).
34. Boehm-Sturm P, Mengler L, Wecker S, Hoehn M, Kallur T. In vivo tracking of human neural stem cells with 19F magnetic resonance imaging. PLoS One. 2011;6(12).
35. Liu L, Ye Q, Wu Y, Hsieh WY, Chen CL, Shen HH, et al. Tracking T-cells in vivo with a new nano-sized MRI contrast agent. Nanomedicine. 2012;8(8).
36. Waiczies H, Lepore S, Janitzek N, Hagen U, Seifert F, Ittermann B, et al. Perfluorocarbon particle size influences magnetic resonance signal and immunological properties of dendritic cells. PLoS One. 2011;6(7).
37. Thorek DLJ, Tsourkas A. Size, charge and concentration dependent uptake of iron oxide particles by non-phagocytic cells. Biomaterials. 2009;29(26).
38. Jain AK, Das M, Swarnakar NK, Jain S. Engineered PLGA nanoparticles: an emerging delivery tool in cancer therapeutics. Critic Rev Therapeut Drug Carrier Syst. 2011;28(1).
39. Luo R, Neu B, Venkatraman SS. Surface functionalization of nanoparticles to control cell interactions and drug release. Small. 2012;8(16).
40. Flaim SF. Pharmacokinetics and side effects of perfluorocarbon-based blood substitutes. Artif Cells Blood Subst Biotechnol. 1994;22(4).
41. Du W, Xu Z, Nyström AM, Zhang K, Leonard JR, Wooley KL. 19F- and fluorescently labeled micelles as nanoscopic assemblies for chemotherapeutic delivery. Bioconjugate Chem. 2008;19(12).
42. Hitchens TK, Ye Q, Eytan DF, Janjic JM, Ahrens ET, Ho C. 19F MRI detection of acute allograft rejection with in vivo perfluorocarbon labeling of immune cells. Magn Reson Med. 2011;65(4).
43. Ruiz-Cabello J, Barnett BP, Bottomley PA, Bulte JW. Fluorine (19F) MRS and MRI in biomedicine. NMR Biomed. 2011;24(2).
44. Maki J, Masuda C, Morikawa S, Morita M, Inubushi T, Matsusue Y, et al. The MR tracking of transplanted ATDC5 cells using fluorinated poly-l-lysine-CF3. Biomaterials. 2007;28(3).
45. Masuda C, Maki Z, Morikawa S, Morita M, Inubushi T, Matsusue Y, et al. MR tracking of transplanted glial cells using poly-l-lysine-CF3. Neurosci Res. 2006;56(2).
46. Bommerich U, Trantzschel T, Mulla-Osman S, Buntkowsky G, Bargon J, Bernarding J. Hyperpolarized 19F-MRI: parahydrogen-induced polarization and field variation enable 19F-MRI at low spin density. Phys Chem Chem Phys. 2010;12(35).